Supporting Information

Wang et al. 10.1073/pnas.1503998112

SI Materials and Methods

Plant Materials and Growth Conditions. *A. thaliana* materials used in this work include the wild-type ecotype Col-0, Landsberg *erecta* (L*er*), and the following mutants or marker lines: *ins-1* (SALK_138654), *ins-2* (GT_5_101747), *trp3-1* (1), *trp3-100* (2), *trp2-1* (3), *trp2-301* (4), *trp5-1* (5), *wei8-1* (6), *yuc4 yuc6* (*yuc4/6*) (7), *sur2* (8), *DR5:GUS* (9), and *DR5:GFP* (10). *Arabidopsis* seeds were surface-sterilized, vernalized at 4 °C for 2–4 d, and germinated on MS medium containing 1.0% (wt/vol) sucrose and 0.6% agar (type M, Sigma-Aldrich) at 21–23 °C in a 16-h light/8-h dark cycle at an intensity of 60–80 $\mu E \cdot m^{-2} \cdot s^{-1}$. For morphological examination, 10-d-old seedlings were transferred to vermiculite saturated with 0.3 × B5 medium and grown under a 16-h light/8-h dark cycle at 21–23 °C as described previously (11). For root observation, seedlings were grown vertically on MS plates containing 2.0% (wt/vol) sucrose and 0.6% phytoagar or on MS plates supplemented with 50 μM Trp for 5 d. The sequences of all of the primers used in this work were listed in Table S1.

Plasmid Construction and Plant Transformation. A 7.7-kb DNA fragment containing the 3-kb upstream sequence, entire *INS* coding region, and 3-kb downstream sequence was amplified by primers INSpro-INS-F and INSpro-INS-R with KpnI and SalI adaptors from the BAC clone T10P11. The amplified DNA fragment was inserted into the KpnI- and SalI-digested pCAMBIA1300 vector (CAMBIA) to generate the complementation construct *INS:INS*, which was transformed into the *ins-1 DR5:GUS* and *ins-1* plants, respectively, by the *Agrobacterium*-mediated floral dip method (12). The T_3 homozygous progeny of *INS:INS*/*ins-1 DR5:GUS* seedlings were used for GUS signal observation, and the T_3 homozygous plants of *INS:INS*/*ins-1* transgenic plants were collected for embryogenesis analysis and quantification of free IAA and Trp contents.

To construct the *35S:TSA* plasmid, a BamHI-KpnI fragment containing the *TSA* coding sequence (CDS) was amplified by primers TSA-OE-F and TSA-OE-R and then subcloned into the BamHI- and KpnI-digested pBin438 vector. To generate the *cTP-INS* fusion fragment, the *cTP* region of *TSA* was amplified by primers G-cTP-F1 and cTP-INS-R1, and the *INS*-coding region was amplified by primers cTP-INS-F2 and G-INS-R2. Then the PCR products were mixed and subjected to an amplification with primers G-cTP-F1 and G-INS-R2. To construct the *35S:ΔcTP-TSA* and *35S:cTP-INS* plasmids, the *ΔcTP-TSA1* fragment amplified from *Arabidopsis* cDNA by primers G-ΔcTP-TSA-F and G-TSA-R and the *cTP-INS* fusion fragment were cloned into the Gateway entry vector pDONR222 (Invitrogen) and subsequently transferred to the binary vector pB7WG2D (13).

To construct the *35S:INS-GFP*, *35S:TSA-GFP*, *35S:cTP-INS-GFP*, and *35S:ΔcTP-TSA-GFP* plasmids, four BamHI-SalI fragments containing *INS* CDS, *TSA* CDS, *cTP-INS*, and *ΔcTP-TSA1* were amplified using primer pairs INS-G-F + INS-G-R, TSA-OE-F +TSA-G-R, cTP-INS-F+ cTP-INS-R, and ΔcTP-TSA-F + ΔcTP-TSA-R, respectively, and then subcloned into BamHI- and SalI-digested pBI221-GFP vector. Recombinant plasmids were subsequently digested with BamHI and EcoRI, and the insertion fragments were subcloned into BamHI- and EcoRI-digested pBI121 vector.

To construct *INS:INS-GFP-GUS* and *TSA:TSA-GFP-GUS* plasmids, the *INSpro:INS* fragment was amplified from the BAC clone T10P11 using primers G-INSpro-F and G-INS no GA-R, and the *TSApro:TSA* fragment was amplified from *Arabidopsis* genomic DNA using primers G-TSApro-F and G-TSA no GA-R. Then *INSpro:INS* and *TSApro:TSA* fragments were cloned into the Gateway entry vector pDONR222 (Invitrogen) and subsequently transferred to the binary vector pBGWFS7 (13).

Gene Expression Analysis. Total RNA was prepared using a TRIzol kit according to the user manual (Invitrogen) and treated with TUBRO DNase (Ambion) before use. First-strand cDNA was synthesized using the oligo(dT) primer with the SSIII first-strand synthesis system (Invitrogen). Real-time PCR experiments were performed using gene-specific primers in a total volume of 20 μL with 1 μL of diluted cDNA, 0.5 μM gene-specific primers, and 10 μL EvaGreen supermix (BioRad) on a CFX 96 real-time system (BioRad) according to the manufacturer's instructions. The *Arabidopsis Ubiquitin5* (*UBQ5*) and *EF1a* genes were used as the internal controls.

Hypocotyl Measurements. Seedlings were grown on MS plates at 20 °C and 28 °C for 9 d in continuous light as previously described (14). Hypocotyl length was measured using ImageJ software (rsbweb.nih.gov/ij/).

Histological and Microscopy Analyses. Histochemical staining for GUS activities was performed as described (15). Briefly, whole seedlings or various tissues were immersed in the GUS staining solution, which contains 2 mM 5-bromo-4-chloro-3-inolyl-β-D-glucuronic acid, 100 mM sodium phosphate (pH 7.2), 10 mM ethylene diamine tetraacetic acid, 0.5 mM potassium ferricyanide, 0.5 mM potassium ferrocyanide, and 0.1% Triton X-100. Plant materials were vacuumed briefly and incubated at 37 °C in dark from 30 min to overnight. The GUS stain solution was removed and replaced with 70% (vol/vol) ethanol to remove chlorophyll from the tissue. *Arabidopsis* roots were then cleared in the HCG solution (chloroacetaldehyde:water:glycerol = 8:3:1) for several minutes before observation. Finally, the GUS signals were observed under a stereomicroscope or microscope, and individual representative seedlings were photographed with a CCD camera.

To observe the subcellular localization of INS-GFP, TSA-GFP, cTP-INS-GFP, and ΔcTP-TSA-GFP, leaves of the stable *35S:INS-GFP*, *35S:TSA-GFP*, *35S:cTP-INS-GFP*, and *35S:ΔcTP-TSA-GFP* transgenic plants were collected for protoplast preparation as described (16). The GFP signals and chlorophyll autofluorescence were examined under a confocal microscope (FluoView FV1000; Olympus) at an excitation wavelength of 488 and 647 nm, respectively.

To observe GFP signals in embryos, ovules were collected in 10% (vol/vol) glycerol solution, and embryos were squeezed out of the ovules by careful extrusion under a cover glass. The GFP signals were examined under a confocal microscope (FluoView FV1000; Olympus) at an excitation wavelength of 488 nm.

To study the development of embryos, siliques were dissected with hypodermic needles and cleared in Herr's solution containing lactic acid:chloral hydrate:phenol:clove oil:xylene (2:2:2:2:1, wt/wt) (17) and observed with a confocal microscope (FluoView 1000; Olympus).

Free IAA Measurement in Seedlings and Aerial Parts. Seedlings of 12-d-old Col-0, *ins-1*, *trp3-1*, *INS:INS*/*ins-1*, *35S:cTP-INS*/*trp3-1*, *INS:INS*/*trp3-1*, *trp2-1*, *ins-1 trp2-1*, *yuc4 yuc6* (*yuc4/6*), *ins-1 yuc4/6*, L*er*, and *ins-2* grown on MS medium were collected and frozen in liquid nitrogen. In addition, aerial parts of 30-d-old Col-0, *ins-1*, *trp2-301*, *ins-1 trp2-301*, *trp2-1*, and *ins-1 trp2-1* plants were used for free IAA measurement. Five or six independent replicates were prepared. For each replicate, ∼200 mg (fresh weight)

materials were homogenized under liquid nitrogen, weighted, and extracted at −20 °C for 24 h with 2 mL of cold methanol containing antioxidant and $^{2}H_2$-IAA (internal standard, CDN Isotopes). Purification was performed with Oasis MAX solid-phase extract cartridge (150 mg/6 cc; Waters). Measurement of free IAA was carried out using a UPLC-MS/MS system consisting of a UPLC system (ACQUITY UPLC; Waters) and a triple quadruple tandem mass spectrometer (Quattro Premier XE; Waters) as previously described (18).

Free IAA Measurement in Ovules. Ovules in the fourth and fifth siliques of the *Arabidopsis* main stem were harvested from the funicle carefully with hypodermic needles and hybrid tweezers and collected in 2.0-mL safe-lock tubes with 200 μL of cold methanol-containing antioxidant. The wild-type ovules, morphologically normal ovules of *ins-1* (*ins-1* normal), and *trp3-1* ovules were light green, whereas the abnormal ovules from the *ins-1* siliques (*ins-1* abnormal) and from the *ins-1 trp3-1*$^{+/-}$ siliques (*ins-1 trp3-1*) were white. Five independent replicates were prepared. Each replicate contained about 80 ovules and 0.2 ng $^{13}C_6$-IAA (internal standard, Cambridge Isotope Laboratories). Then samples were homogenized by ball mill (MM 400; Retsch GmbH) at a frequency of 28 Hz for 1 min using 3-mm tungsten carbide beads. After extraction at −20 °C for 12 h, the samples were centrifuged at 16,000 × *g* for 15 min, and the supernatants were collected and dried with nitrogen. The residues were derivatized with bromocholine bromide (BETA, TCI) as previously described (19). After evaporation of the reaction mixture, the residues were reconstituted and subjected to solid-phase extraction with Bond Elut CBA cartridges (1 mL, Agilent) for further enrichment. After evaporation, the residues were dissolved with 300 μL of 10% (vol/vol) acetonitrile containing 0.1% formic acid. The IAA derivative was analyzed using the UPLC-MS/MS system consisting of a UPLC (ACQUITY UPLC) and a triple quadruple tandem mass spectrometer (QTRAP 5500; AB SCIEX) under positive ion mode. Chromatographic separation was performed on an ACQUITY UPLC BEH C_{18} column (100 × 2.1 mm, 1.7 μm; Waters) with the column temperature set at 25 °C, and the flow rate was 0.4 mL/min. The linear gradient runs from 88 to 66% (vol/vol) A (solvent A, 0.1% formic acid aqueous; solvent B, acetonitrile) in 7 min and from 66–8% (vol/vol) A in the next 1 min and is re-equilibrated with the initial condition for 3 min. The optimized mass spectrometer parameters were set as follows: curtain gas 20 psi, collision gas 6 psi, ion spray voltage 5,450 V, temperature 600 °C. The declustering potential (93 V) and collision energy (42 V) were applied. Multiple reaction monitoring (MRM) mode was used for quantification and the selected MRM transitions were 261.0 > 130.0 for IAA derivative and 267.0 > 136.0 for $^{13}C_6$-IAA derivative, respectively.

$^{13}C_6$-IAA Measurement in Seedlings. Five independent replicates were collected for $^{13}C_6$-IAA quantification. For each replicate, ∼400 mg (fresh weight) whole seedlings were homogenized under liquid nitrogen, weighted, and extracted for 24 h with 3 mL of cold methanol-containing antioxidant and 2.5 ng $^{2}H_2$-IAA (internal standard, CDN Isotopes). Endogenous $^{13}C_6$-IAA produced from $^{13}C_6$-anthranilic acid was measured similarly to that previously described (18) with some changes under UPLC-MS/MS conditions. The UPLC-MS/MS system consisted of a UPLC (ACQUITY UPLC) and a tandem mass spectrometer (QTRAP 5500). The chromatographic separation was achieved on an ACQUITY UPLC BEH C_{18} column (50 × 2.1 mm, 1.7 μm; Waters) with the column temperature at 30 °C and a flow rate of 0.2 mL/min. The linear gradient runs from 90 to 60% (vol/vol) A (solvent A, 0.05% acetic acid aqueous; solvent B, methanol) in 4 min, 60–35% (vol/vol) A in the next 4 min, 35–2% (vol/vol) A in the following 1 min and is re-equilibrated with the initial condition for 2 min. The optimized mass spectrometer parameters were set as follows: curtain gas at 40 psi, collision gas at 6 psi, ion spray voltage at −4,300 V, and temperature at 550 °C. The declustering potential (−85 V) and collision energy (−13 V) were applied. MRM mode was used for quantification and the selected MRM transitions were 180.1 > 136.1 for $^{13}C_6$-IAA and 176.1 > 132.0 for $^{2}H_2$-IAA.

Endogenous Trp Measurement. Seedlings of 7-d-old Col-0, *ins-1*, *trp3-1*, *trp2-1*, *35S:TSA*/*trp3-1*, *35S:cTP-INS*/*trp3-1*, *INS:INS*/*ins-1*, and *trp5-1* grown on MS medium were collected for Trp measurement. Frozen seedling samples were homogenized under liquid nitrogen. The fine powder of lyophilized tissues (6.0 mg) was transferred into a 4-mL glass vial. Then 1.5 mL of chloroform was added to the dry tissues. The sample was thoroughly vortexed and incubated for 45 min at 37 °C. After cooling down to room temperature, 1.5 mL of HPLC-grade water containing 3 μg $^{2}H_5$-Trp (internal standard, Sigma-Aldrich) was added to the chloroform. Then the sample was vortexed, incubated for 45 min at 37 °C, and centrifuged at 3,000 × *g* for 30 min to separate the phases. Then 1.0 mL of aqueous phase was transferred into a 1.5-mL tube and lyophilized to dry. The dry residue was resuspended into 50 μL of pyridine containing 15.0 mg/mL methoxyamine–HCl and incubated for 1 h at 50 °C after a brief sonication. Metabolites were then directly derivatized by mixing 50 μL of *N*-methyl-*N*-(trimethylsilyl) trifluoroacetamide (MSTFA) with 1% trimethylchlorosilane (TMCS) (MSTFA + 1% TMCS, Fluka, 69478) for 1 h at 50 °C. The clear supernatant was transferred into a glass insert after centrifugation at 20,000 × *g* for 10 min, and 1 μL of supernatant was loaded on a gas chromatography-tandem mass spectrometry (GC-MS) system (Trace DSQ II; Thermo Fisher company) equipped with a 30-M DB 5MS column for Trp measurement. The oven temperature program was initially set at 150 °C for 1 min and then ramped to 240 °C at 20 °C/min, to 260 °C at 10 °C/min, and to 300 °C at 20 °C/min and and held for 5 min. The signal was collected using the SIM mode. The intensity of *m*/*z* 202 and 207, corresponding to Trp and $^{2}H_5$-Trp (retention time 19.59 min), respectively, was used for endogenous Trp calculation.

Genetic Analysis. Double and triple mutants were generated from the crosses of relevant homozygous single or double mutants and identified from the F_2 progenies. Genotyping of the *ins-1*, *ins-2*, *wei8-1*, *sur2*, *yuc4*, *yuc6*, *trp3-1*, *trp3-100*, *trp2-1*, *trp2-301*, and *trp5-1* mutants was performed by PCR using the primers in Table S1. In detail, the PCR products of the wild type and *trp3-1* amplified by primers *trp3-1*-F ad *trp3-1*-R were digested with BslI. The PCR products of the wild type and *trp3-100* amplified by primers *trp3-100*-F and *trp3-100*-R were digested with FokI. The PCR products of the wild type and *trp2-1* amplified by primers of *trp2-1*-F and *trp2-1*-R were digested with BseRI. The PCR products of the wild-type and *trp2-301* amplified by primers of *trp2-1*-F and *trp2-1*-R were digested with BglII. The PCR products of the wild-type and *trp5-1* amplified by primers of *trp5-1*-F and *trp5-1*-R were digested with PstI. The *ins-1* mutant was genotyped using primer pairs 654RP + LBb1 and 326RP + 326LP. The *ins-2* mutant was genotyped using primer pairs 537G03RP + Ds5-4 and 537G03LP + 537G03RP. The *wei8-1* mutant was genotyped using primer pairs 70560R1 + DWLB1 and 70560F8 + 70560R1. The *sur2* mutant was genotyped using primer pairs 028573RP + LBb1 and 028573LP + 028573RP. The *yuc4* mutant was genotyped using primer pairs YUC4-R + SMP32 and YUC4-F + YUC4-R. The *yuc6* mutant was genotyped using primer pairs YUC6-R + LBb1 and YUC6-F + YUC6-R.

1. Last RL, Fink GR (1988) Tryptophan-requiring mutants of the plant *Arabidopsis thaliana*. *Science* 240(4850):305–310.

2. Radwanski ER, Barczak AJ, Last RL (1996) Characterization of tryptophan synthase alpha subunit mutants of *Arabidopsis thaliana*. *Mol Gen Genet* 253(3):353–361.

3. Last RL, Bissinger PH, Mahoney DJ, Radwanski ER, Fink GR (1991) Tryptophan mutants in *Arabidopsis*: The consequences of duplicated tryptophan synthase beta genes. *Plant Cell* 3(4):345–358.
4. Jing Y, et al. (2009) Tryptophan deficiency affects organ growth by retarding cell expansion in Arabidopsis. *Plant J* 57(3):511–521.
5. Li J, Last RL (1996) The *Arabidopsis thaliana trp5* mutant has a feedback-resistant anthranilate synthase and elevated soluble tryptophan. *Plant Physiol* 110(1):51–59.
6. Stepanova AN, et al. (2008) TAA1-mediated auxin biosynthesis is essential for hormone crosstalk and plant development. *Cell* 133(1):177–191.
7. Cheng Y, Dai X, Zhao Y (2006) Auxin biosynthesis by the YUCCA flavin monooxygenases controls the formation of floral organs and vascular tissues in *Arabidopsis*. *Genes Dev* 20(13):1790–1799.
8. Barlier I, et al. (2000) The *SUR2* gene of *Arabidopsis thaliana* encodes the cytochrome P450 CYP83B1, a modulator of auxin homeostasis. *Proc Natl Acad Sci USA* 97(26):14819–14824.
9. Ulmasov T, Murfett J, Hagen G, Guilfoyle TJ (1997) Aux/IAA proteins repress expression of reporter genes containing natural and highly active synthetic auxin response elements. *Plant Cell* 9(11):1963–1971.
10. Benková E, et al. (2003) Local, efflux-dependent auxin gradients as a common module for plant organ formation. *Cell* 115(5):591–602.
11. Mou Z, He Y, Dai Y, Liu X, Li J (2000) Deficiency in fatty acid synthase leads to premature cell death and dramatic alterations in plant morphology. *Plant Cell* 12(3):405–418.
12. Clough SJ, Bent AF (1998) Floral dip: A simplified method for *Agrobacterium*-mediated transformation of *Arabidopsis thaliana*. *Plant J* 16(6):735–743.
13. Karimi M, Inzé D, Depicker A (2002) GATEWAY vectors for *Agrobacterium*-mediated plant transformation. *Trends Plant Sci* 7(5):193–195.
14. Gray WM, Ostin A, Sandberg G, Romano CP, Estelle M (1998) High temperature promotes auxin-mediated hypocotyl elongation in *Arabidopsis*. *Proc Natl Acad Sci USA* 95(12):7197–7202.
15. Jefferson RA, Kavanagh TA, Bevan MW (1987) GUS fusions: Beta-glucuronidase as a sensitive and versatile gene fusion marker in higher plants. *EMBO J* 6(13):3901–3907.
16. Sheen J (2001) Signal transduction in maize and Arabidopsis mesophyll protoplasts. *Plant Physiol* 127(4):1466–1475.
17. Herr JM (1971) A new clearing-squash technique for the study of ovule development in angiosperms. *Am J Bot* 58(8):785–790.
18. Fu J, Chu J, Sun X, Wang J, Yan C (2012) Simple, rapid, and simultaneous assay of multiple carboxyl containing phytohormones in wounded tomatoes by UPLC-MS/MS using single SPE purification and isotope dilution. *Anal Sci* 28(11):1081–1087.
19. Sun X, et al. (2014) An in-advance stable isotope labeling strategy for relative analysis of multiple acidic plant hormones in sub-milligram *Arabidopsis thaliana* seedling and a single seed. *J Chromatogr A* 1338:67–76.

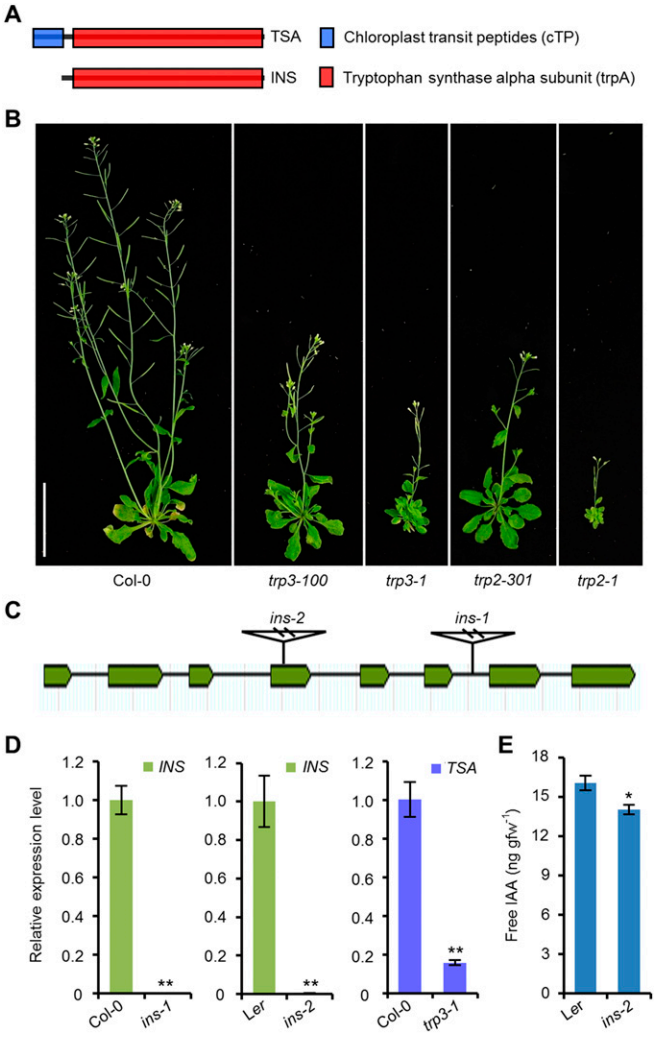

Fig. S1. Identification of *ins* and *trp3* mutants. (*A*) Domains of TSA and INS. INS lacks the chloroplast transit peptides (cTP). (*B*) Phenotypes of wild-type (Col-0), *trp3*, and *trp2* plants. The *trp3* and *trp2* mutants display typical Trp auxotrophic phenotypes compared with the wild type, for example, growing more slowly, exhibiting light-conditional phenotypes, and dwarf. The *trp3-100* mutant is a weak allele of *TSA* and *trp2-301* is a weak allele of *TSB1*. (Scale bar, 5 cm.) (*C*) Schematic diagram of the T-DNA insertion sites of *ins-1* and *ins-2*. The *ins-1* (SALK_138654) and *ins-2* (GT_5_101747) lines carry T-DNA insertions in intron 6 and in exon 4, respectively. (*D*) Relative expression levels of *INS* and *TSA*. *INS* is knocked out in both *ins-1* and *ins-2*, whereas *TSA* is knocked down in *trp3-1*. Data are represented as mean ± SEM; $^{**}P < 0.01$ by Student's *t* test; $n = 3$. (*E*) Free IAA contents of 12-d-old wild-type (*Ler*) and *ins-2* seedlings. gfw^{-1}, per gram fresh weight. Data are represented as mean ± SEM; $^{*}P < 0.05$ by Student's *t* test; $n = 4$.

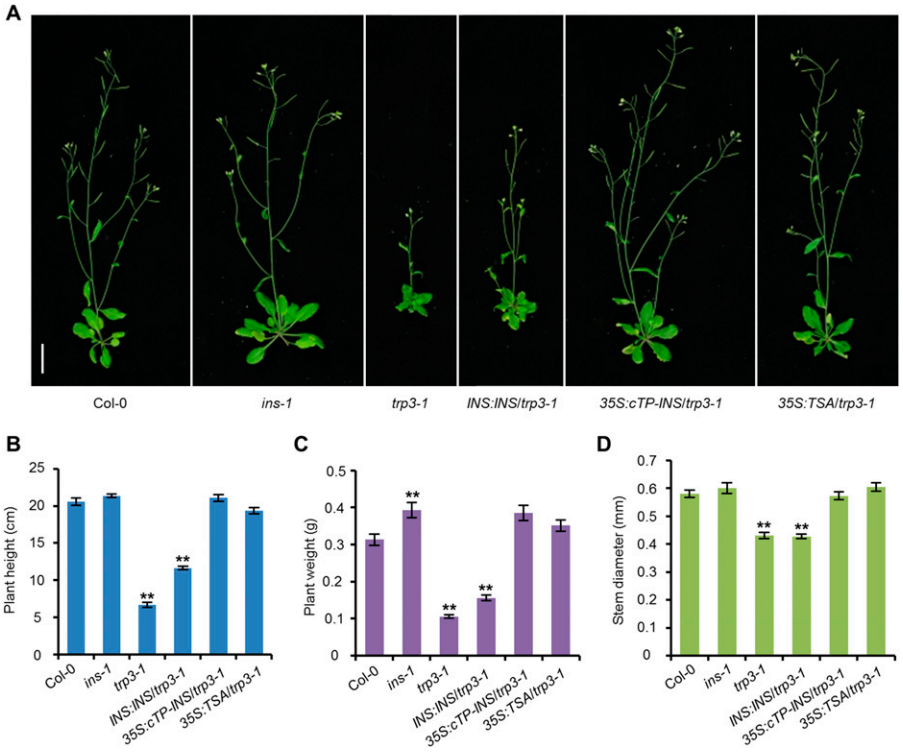

Fig. S2. Morphological comparison among wild-type (Col-0), *ins-1*, *trp3-1*, *INS:INS/trp3-1*, *35S:cTP-INS/trp3-1*, and *35S:TSA/trp3-1* plants. (*A*) Phenotypes of 40-d-old plants. (Scale bar, 2 cm.) (*B–D*) Quantitative analyses of plant height (*B*), plant fresh weight (*C*), and stem diameter (*D*) in 40-d-old plants. Data are represented as mean ± SEM; $^{**}P < 0.01$ by Student's *t* test; $n = 20$.

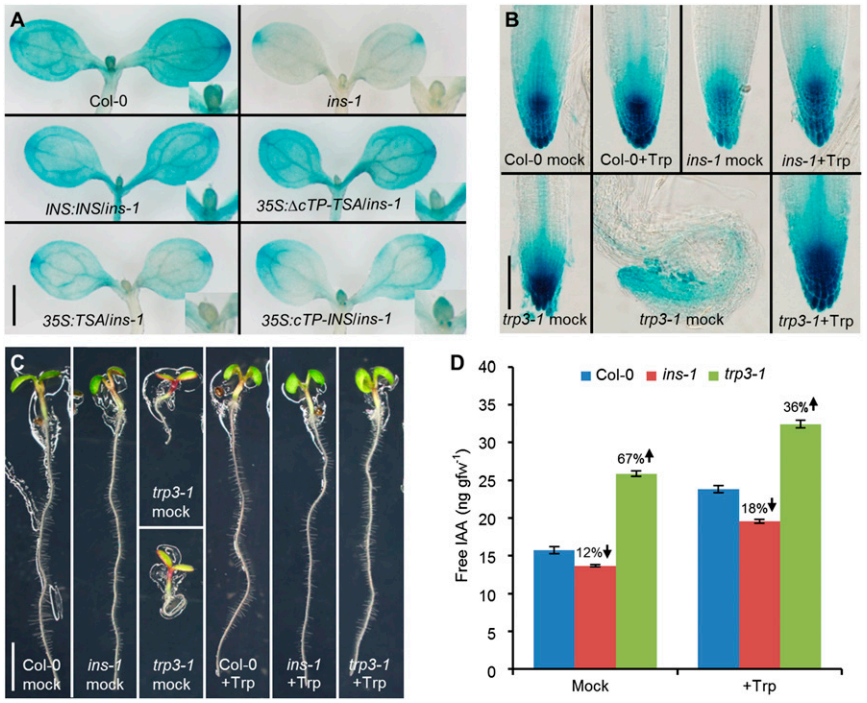

Fig. S3. Observations of *DR5* activities and effects of Trp treatment on wild-type, *ins-1*, and *trp3-1* seedlings. (*A*) The *DR5* activities visualized by GUS signals in 5-d-old wild-type (Col-0), *ins-1*, *INS:INS/ins-1*, *35S:ΔcTP-TSA/ins-1*, *35S:TSA/ins-1*, and *35S:cTP-INS/ins-1* seedlings. (*Insets*) Enlarged shoot tips. Overexpression of *INS* and *ΔcTP-TSA* rescued the *DR5* activity of *ins-1*. (*B* and *C*) Expression patterns of *DR5:GUS* reporters (*B*) and morphologies (*C*) of 5-d-old wild-type (Col-0), *ins-1*, and *trp3-1* seedlings grown with or without 50 μM Trp supplement. The *trp3-1* seedlings displayed short and curved roots with disordered expression patterns of *DR5:GUS*. (*D*) Free IAA contents in 12-d-old Col-0, *ins-1*, and *trp3-1* seedlings grown with or without 50 μM Trp supplement. gfw^{-1}, per gram fresh weight. Data are represented as mean ± SEM; $n = 5$. (Scale bars, 1 mm in *A*, 0.1 mm in *B*, and 0.2 cm in *C*.)

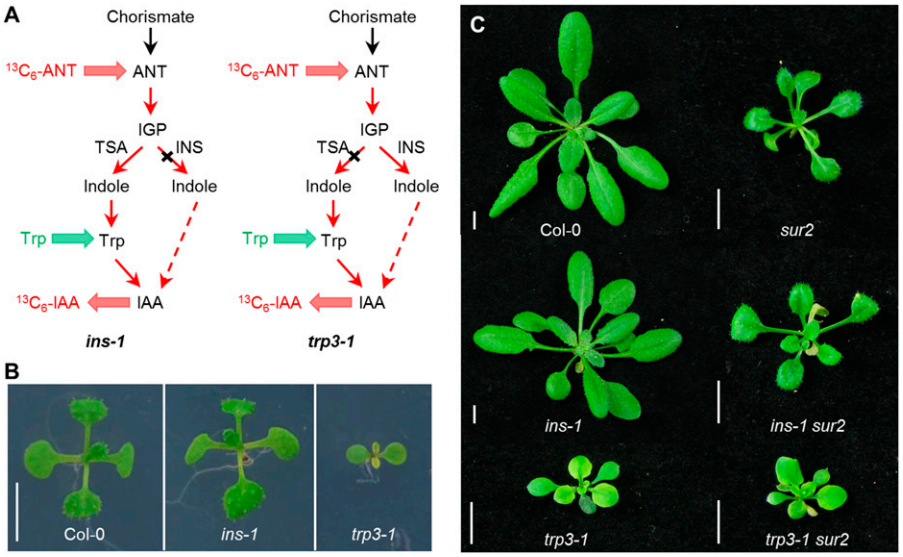

Fig. S4. Plant materials of $^{13}C_6$-anthranilic acid feeding experiment and phenotypic analysis of the *ins-1 sur2* and *trp3-1 sur2* double mutants. (*A*) Schematic diagrams of $^{13}C_6$-anthranilic acid ($^{13}C_6$-ANT) feeding experiment. The 11-d-old wild-type (Col-0), *ins-1*, and *trp3-1* seedlings were transferred to liquid MS media containing 64 μM $^{13}C_6$-ANT and cultured for 24 h at 28 °C. In a parallel test, the MS medium contained 64 μM $^{13}C_6$-ANT and 100 μM unlabeled Trp, which should increase the Trp pool size and decrease the biosynthesis of $^{13}C_6$-IAA only through the Trp-dependent pathway. (*B*) Morphologies of 11-d-old Col-0, *ins-1*, and *trp3-1* seedlings used for $^{13}C_6$-ANT feeding experiment. The *trp3-1* mutant formed small and yellow true leaves. (*C*) Phenotypes of 30-d-old wild-type (Col-0), *ins-1*, *sur2*, *ins-1 sur2*, *trp3-1*, and *trp3-1 sur2* plants. The phenotypes of *sur2* were suppressed by *trp3-1*, but not by *ins-1*. (Scale bars, 0.5 cm in *B* and *C*.)

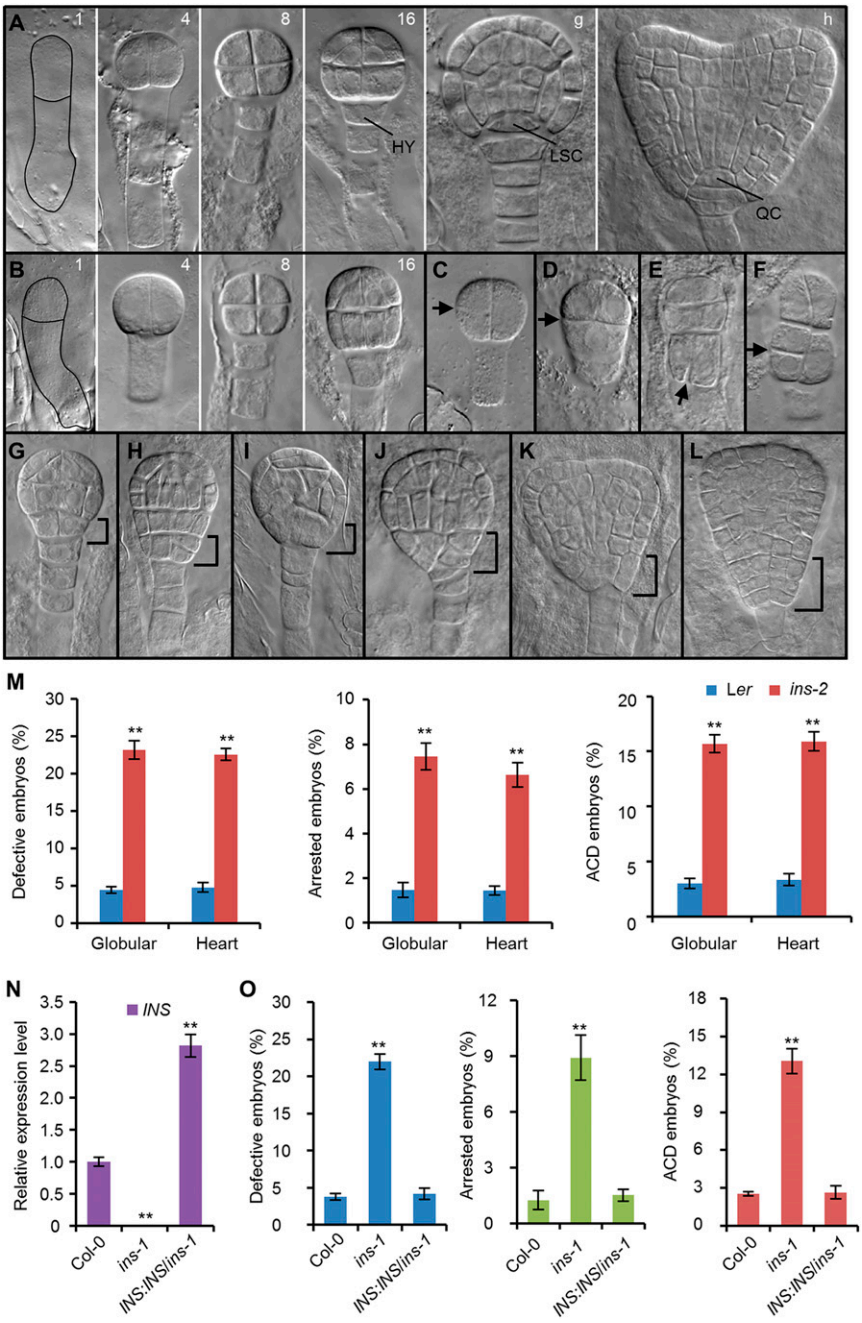

Fig. S5. Embryogenesis of *ins-2* and *INS:INS/ins* transgenic plants. (*A*) Embryos of wild-type (L*er*) at the 1-, 4-, 8- or 16-cell, globular (g), and heart (h) stages. HY, hypophysis; LSC, lens-shaped cell; and QC, quiescent center. (*B*–*L*) Defective embryos of *ins-2* arrested with correct body plans (*B*) or displayed abnormal cell division patterns (*C*–*L*) when normal sibling embryos reached the heart stage. The root meristems (*G*–*L*) and cotyledon primordia (*K* and *L*) were aberrant. Arrows indicate abnormal cell plates at wrong positions or in wrong orientations, and brackets mark aberrant basal cell regions. (*M*) Statistical analysis of embryonic defects in L*er* and *ins-2*. (*N*) Relative expression levels of *INS* in wild-type (Col-0), *ins-1*, and *INS:INS/ins-1* plants. Data are represented as mean ± SEM; $^{**}P < 0.01$ by Student's *t* test; $n = 3$. (*O*) Statistical analysis of embryonic defects in Col-0, *ins-1*, and *INS:INS/ins-1* plants. In *M* and *O*, the percentage of defective embryos, arrested embryos with correct body plans, and embryos with abnormal cell division planes (ACD) are analyzed. Data are represented as mean ± SEM; $^{**}P < 0.01$ by Student's *t* test; $n = 4$, and each biological repeat contains about 200 embryos.

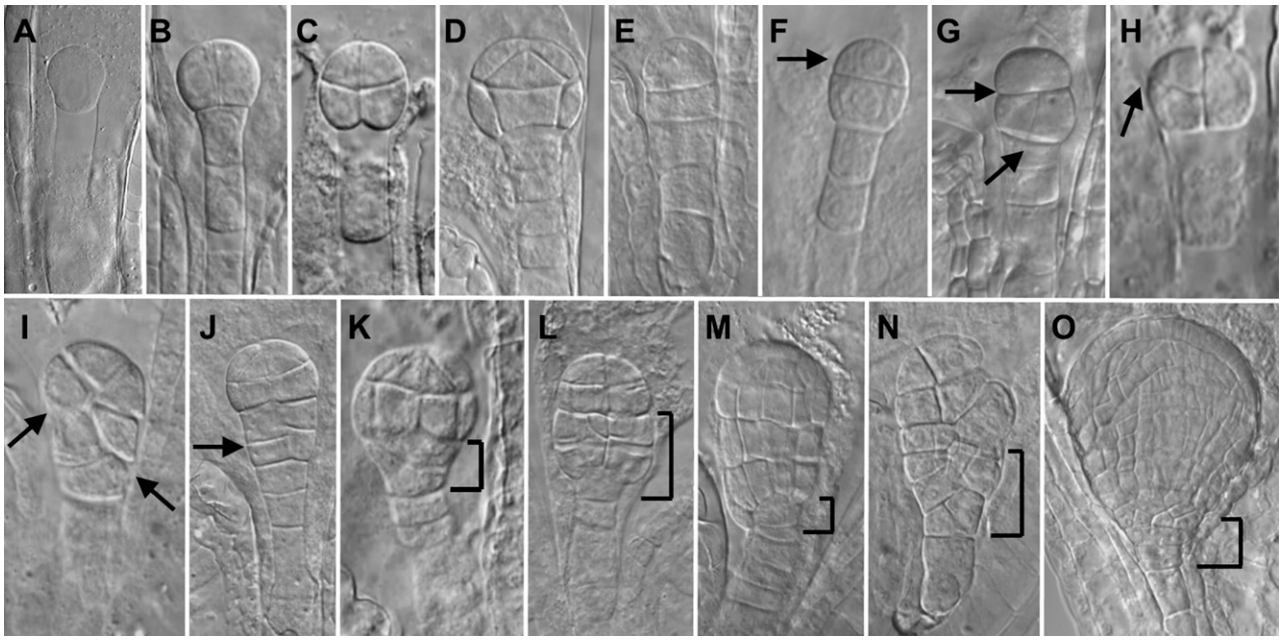

Fig. S6. Embryogenesis of the *ins-1 trp3-100* double mutant. (*A*–*O*) When normal sibling embryos reached the heart stage, defective embryos from *ins-1 trp3-100*$^{+/-}$ siliques arrested at the 1- (*A*), 4- (*B*), 8- (*C*) or 16-cell *(D)* stage with regular cell division patterns or displayed abnormal cell division planes (*E*–*O*). For example, defective embryos formed filamentous structure without specification of a proembryo (*E*), possessed an apical cell with transverse division (*F* and *G*), underwent incomplete transverse division (*H*), exhibited disordered polarity at the eight-cell stage (*I*), formed additional layers of cells in the proembryo (*K*), and lacked root meristem and cotyledon primordia (*K*–*O*). Arrows indicate abnormal cell plates at wrong positions or in wrong orientations, and brackets mark aberrant basal cell regions.

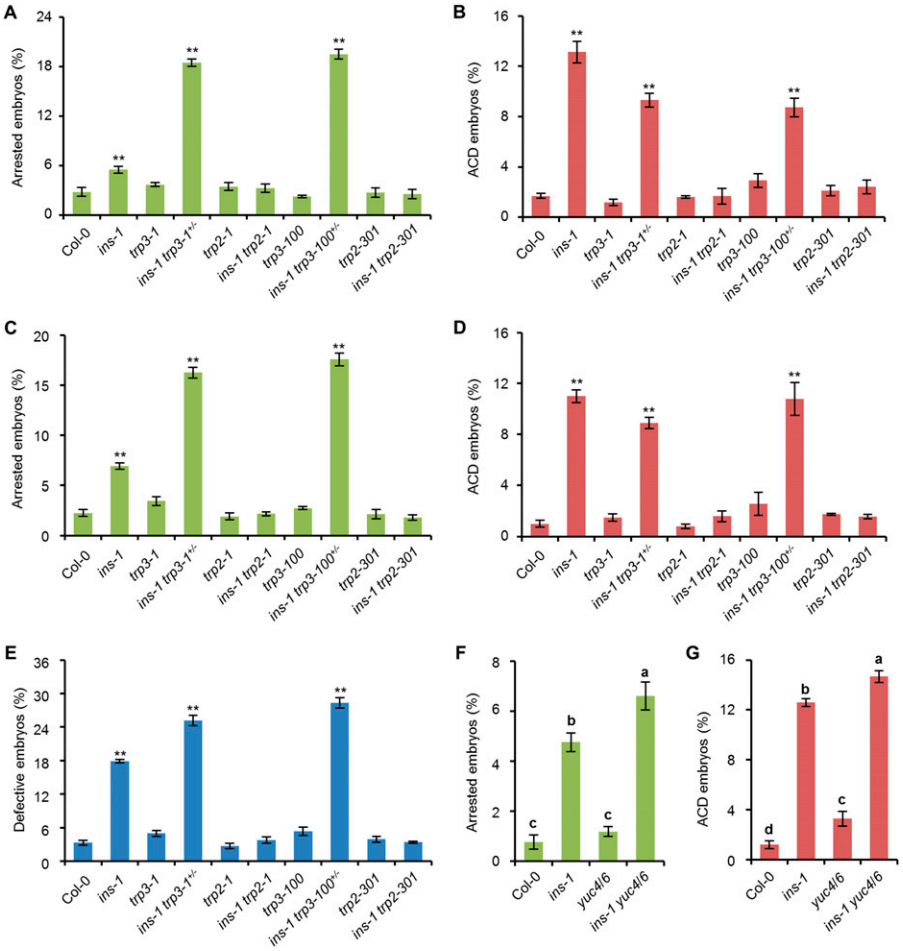

Fig. S7. Statistical analyses of embryonic defects in Col-0, *ins-1*, *trp3*, *ins-1 trp3*$^{+/-}$, *trp2*, *ins-1 trp2*, *yuc4/6*, and *ins-1 yuc4/6* plants. (*A* and *B*) Percentages of arrested embryos (*A*) and ACD embryos (embryos with abnormal cell division planes) (*B*) in the wild-type (Col-0) and mutants at the globular stage. (*C*–*E*) Percentages of arrested embryos (*C*), ACD embryos (*D*), and defective embryos (*E*) in the wild-type (Col-0) and mutants at the heart stage. (*A*–*E*) Data are represented as mean ± SEM; $^{**}P < 0.01$ by Student's *t* test; $n = 4$, and each biological repeat contains about 250 embryos. (*F* and *G*) Percentages of arrested embryos (*F*) and ACD embryos (*G*) in wild type (Col-0), *ins-1*, *yuc4/6*, and *ins-1 yuc4/6* at the globular stage. Data are represented as mean ± SEM; different letters indicate significant difference by Tukey's multiple comparison test ($P < 0.05$); $n = 4$, and each biological repeat contains about 250 embryos.

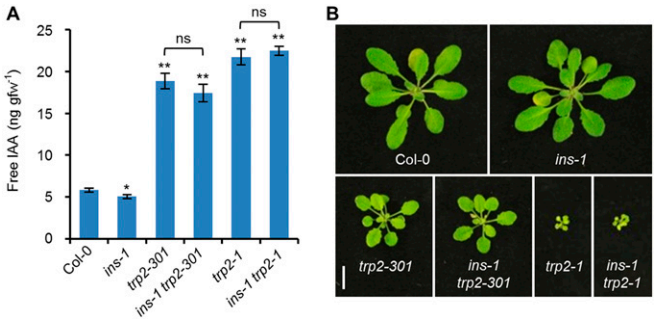

Fig. S8. Comparisons of IAA contents and morphologies among *ins-1*, *trp2*, and their double mutants. (*A*) Free IAA content in 30-d-old Col-0 ($n = 5$), *ins-1* ($n = 6$), *trp2-301* ($n = 5$), *ins-1 trp2-301* ($n = 6$), *trp2-1* ($n = 6$), and *ins-1 trp2-1* ($n = 6$) plants. gfw^{-1}, per gram fresh weight; ns, no significant difference. Data are represented as mean ± SEM; $^{*}P < 0.05$ and $^{**}P < 0.01$ by Student's *t* test. (*B*) Phenotypes of 4-wk-old wild-type (Col-0), *ins-1*, *trp2-301*, *ins-1 trp2-301*, *trp2-1*, and *ins-1 trp2-1* plants. (Scale bar, 1 cm.)

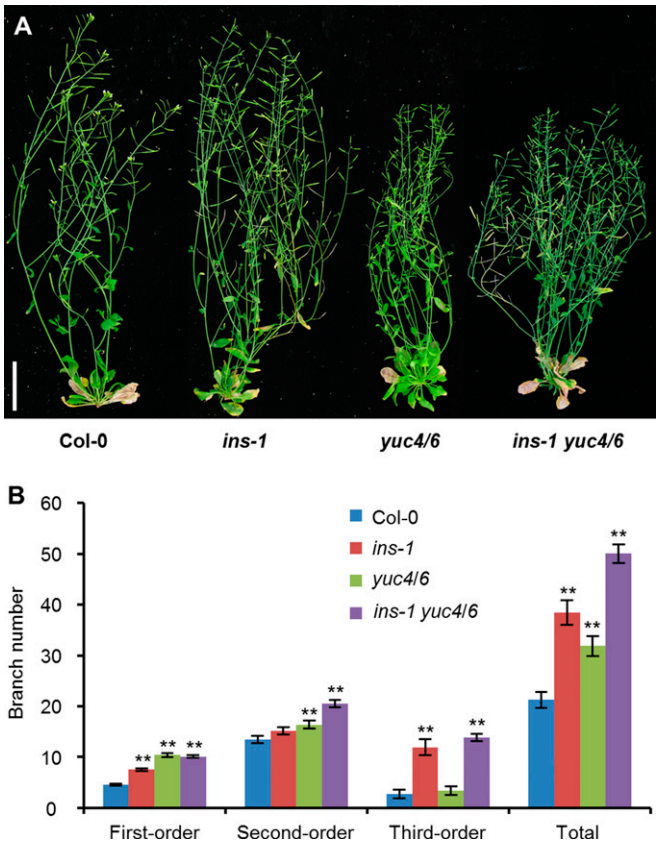

Fig. S9. INS and YUCs cooperatively regulate shoot branching. (*A*) Phenotypes of 7-wk-old Col-0, *ins-1*, *yuc4/6*, and *ins-1 yuc4/6* plants. (Scale bar, 4 cm.) (*B*) Quantitative analysis of branch number per plant. Data are represented as mean ± SEM; $^{**}P < 0.01$ by Student's *t* test; $n = 30$.

Table S1. Primers used in this study

Primer name	Sequence
Primers for plasmid construction	
INSpro-INS-F	5′-aaggtaccATGTTGTTGTTAATAGTGGACCAATT-3′
INSpro-INS-R	5′-aagtcgacTCCAATAGCTTCGACTTCGACTT-3′
TSA-OE-F	5′-ggatccATGGCGATTGCTTTCAAA-3′
TSA-OE-R	5′-atggtaccTCAAAGAAGAGCAGATTTAAGA-3′
INS-G-F	5′-ggatccATGGATCTTCTCAAGACTCCTT-3′
INS-G-R	5′-gtcgacAGAGACAAGAGCAGACTTCAAAG-3′
TSA-G-R	5′-gtcgacAAGAAGAGCAGATTTAAGAGACTTG-3′
cTP-INS-F	5′-ttcggatccATGGCGATTGCTTTCAAA-3′
cTP-INS-R	5′-tttgtcgacAGAGACAAGAGCAGACTTC-3′
ΔcTP-TSA-F	5′-ttaggatccATGGCTTCTCTCTCCACC-3′
ΔcTP-TSA-R	5′-tccgtcgacAAGAAGAGCAGATTTAAGAGA-3′
G-cTP-F1	5′-GGGGACAAGTTTGTACAAAAAAGCAGGCTTAATGGCGATTGCTTTCAAA-3′
cTP-INS-R1	5′-GAGGAAGGAGTCTTGAGAAGATCCATGGGAGTGAATCTCTTGAAAGAAAGCGATG-3′
cTP-INS-F2	5′-CATCGCTTTCTTTCAAGAGATTCACTCCCATGGATCTTCTCAAGACTCCTTCCTC-3′
G-INS-R2	5′-GGGGACCACTTTGTACAAGAAAGCTGGGTATCAAGAGACAAGAGCAGA-3′
G-ΔcTP-TSA-F	5′-GGGGACAAGTTTGTACAAAAAAGCAGGCTTAATGGCTTCTCT CTCCACC-3′
G-TSA-R	5′-GGGGACCACTTTGTACAAGAAAGCTGGGTATCAAAGAAGAGCAG ATTT-3′
G-INSpro-F	5′-GGGGACAAGTTTGTACAAAAAAGCAGGCTTATACATACGGCTT CGACTC-3′
G-INS no GA-R	5′-GGGGACCACTTTGTACAAGAAAGCTGGGTAAAGAGACAAGAGCAGACT-3′
G-TSApro-F	5′-GGGGACAAGTTTGTACAAAAAAGCAGGCTTATCAGGTTTGTCA AATACC-3′
G-TSA no GA-R	5′-GGGGACCACTTTGTACAAGAAAGCTGGGTAAAAGAAGAGCAGATTTAA-3′
Primers for genotyping	
654RP	5′-CCTTGCTCAGGTGATTCAGAC-3′
326LP	5′-CTGCGACGAGGAGTAGAGAAC-3′
326RP	5′-TTCGGAACCCGAAAATCTAC-3′
537G03LP	5′-GACTCGCCCAAGATCTTAACC-3′
537G03RP	5′-TGATCCATTAGCTGATGGTCC-3′
YUC4-F	5′-TTGTCAAACCGAGGCGTACC-3′
YUC4-R	5′-ACGACCATATGAGGCAGAGC-3′
YUC6-F	5′-TCTGCAACTTCGGTGCTCAG-3′
YUC6-R	5′-TTTAACGAGAACATCTTAAAGCGCTG-3′
70560F8	5′-CATCAGAGAGACGGTGGTGAAC-3′
70560R1	5′-GCTTTTAATGAGCTTCATGTTGG-3′
028573LP	5′-TTTCGTGGTTCTCTCTTTTCG-3′
028573RP	5′-GTGGTATGGGCCATGACTTAC-3′
trp3-1-F	5′-ATGTGTGTTTGTGTCCCCTGTCA-3′
trp3-1-R	5′-CTCCCCATCCAGCTATCTGTTG-3′
trp3-100-F	5′-GAATACTCTTGGCTGGTAGATTTCA-3′
trp3-100-R	5′-TGTGGAACAACCTGCACCAA-3′
trp2-1-F	5′-CCTGGAGTCGGACCCGAGCA-3′
trp2-1-R	5′-TGTTGGAAACGTACTGACCAGAGAG-3′
trp5-1-F	5′-ACGTTTTGAGCGGCGAACATCTGCA-3′
trp5-1-R	5′-TGCTTTACTTTGGTGAGAATTTCTG-3′
LBb1	5′-GCGTGGACCGCTTGCTGCAACT-3′
Ds5-4	5′-TACGATAACGGTCGGTACGG-3′
SMP32	5′-TACGAATAAGAGCGTCCATTTTAGAGTGA-3′
DWLB1	5′-CATACTCATTGCTGATCCATGTAGATTTCC-3′
Primers for qPCR	
Q-UBQ5-F	5′-GCTTCATCTCGTCCTCCGTC-3′
Q-UBQ5-R	5′-AGAACAGCGAGCTTAACCTTCTTAT-3′
Q-EF1a-F	5′-TGAGCACGCTCTTCTTGCTTTCA-3′
Q-EF1a-R	5′-GGTGGTGGCATCCATCTTGTTACA-3′
Q-INS-F	5′-ACTGCTCACAACACCCACAACT-3′
Q-INS-R	5′-AACCCCTACTGAACTTACGAGATAGAT-3′
Q-TSA-F	5′-CATTTGCAGACAACATCTTTAGATT-3′
Q-TSA-R	5′-GTGTGGCTTGAGTCACAGTAACTTATT-3′